The Institution of Engineering and Technology

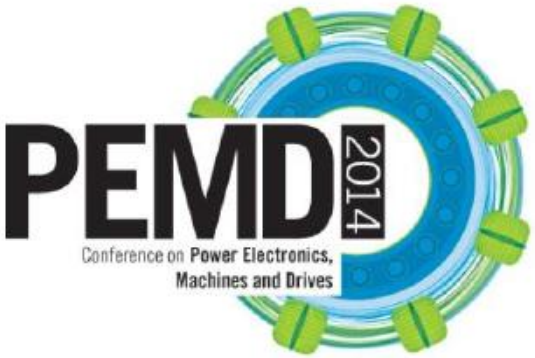

8 - 10 April 2014 | Midland Hotel, Manchester, UK

Tuesday 8 April 2014

Machines and Drives

0040 **FPGA implementation of extended Kalman filter for speed-sensorless control of induction motors**
R Inan[1], M Barut[1], F Karakaya[1], [1]*Nigde University, Turkey*

0056 **Active power reversal in a three phase induction motor connected to a single phase supply**
J Peuteman[1], F Rubben[2], G Van Heerswynghels[2], D Vanoost[1], T Verbeerst[1], W Weyns[1], [1]*KU Leuven Kulab, Belgium,* [2]*Vrij Technisch Instituut Brugge, Belgium*

0079 **Analysis and force computations of single-phase permanent-capacitor induction motors using FEM at broken bar conditions**
H Hanafy[1], T Abdo[1], A Adly[1], [1]*Cairo University, Egypt*

0092 **Traction system with on-board inductive power transfer**
A Abdel-Khalik[1], S Ahmed[2], A Massoud[3], [1]*Alexandria University, Egypt,* [2]*Texas A & M Univ. at Qatar, Qatar,* [3]*Qatar University, Qatar*

0107 **Particle swarm optimization design of air-cored axial flux permanent magnet generator for small-scale wind power systems**
B Xia[1], P C K Luk[1], W Fei[1], L Yu[1], [1]*Cranfield University, UK*

0137 **FPGA-based hierarchical finite-states predictive control of PMSM-IPM drives**
M Carraro[1], L Peretti[2], M Zigliotto[1], [1]*University of Padova, Italy,* [2]*ABB Corporate Research AB, Sweden*

0170 **Torque ripple reduction of radial magnetic gearbox using axail pole pairing**
H Zaytoon[1], A Abdel-Khalik[1], A Massoud[1,2], S Ahmed[3], I Elarabawy[1], [1]*Alexandria University, Egypt,* [2]*Qatar University, Qatar,* [3]*Texas A & M University, Qatar*

0177 **High Efficiency Control of Flux Switching Transverse Flux Permanent Magnet Generator for Wind Generation System**
J Yan[1], H Lin[2], Y Feng[2], H Yang[2], Y Guo[2], [1]*Nanjing University of Science and Technology, China,* [2]*Southeast University, China*

0179 **Optimal Design of the Magnetizing fixture using Taguchi Robust Design in the ring-type PMSM**
S Lee[1], K Kim[1], S Cho[1], J Jang[1], T Lee[1], J Hong[1], [1]*Hanyang University, Republic of Korea*

0197 **Vector controlled five-phase PWM-CSI induction motor drive fed from controlled three-phase PWM current source rectifier**
M Masoud[1], A Abdelkhalik[2], R Al Abri[1], [1]*Sultan Qaboos University, Oman,* [2]*Alexandria University, Egypt*

0204 **Analysis and modelling of rotor eccentricity for switched reluctance machines**
C Weiss[1], A Hofmann[1], R De Doncker[1], [1]*RWTH Aachen University, Germany*

Optimal Design of the Magnetizing fixture using Taguchi Robust Design in the ring-type PMSM

S J Lee, K S Kim, S Cho, J Jang, T H Lee, J P Hong

Department of Automotive Engineering, Hanyang University, Seoul 133-791, Korea

Keywords: Electromotive force, Magnetization, Magnetizing fixture, Permanent Magnet Synchronous motor (PMSM), Taguchi robust design

Abstract

The design the magnetizing fixture is important because the quality of magnetization depends on the design of the magnetizing fixture. Especially, the magnetization direction in the case of ring-type permanent magnet synchronous motor (PMSM) is crucial because the position or the structure of PM cannot be modified. Moreover, the uncertain magnetization of the PM occurs fairly often in the ring-type PMSM in industry. Therefore, this paper presents a Taguchi robust design of the surface flux density characteristic analysis using the structural optimization of magnetizing fixture in order to optimize the magnetization in the PM. The validity of the analysis method is verified by test.

1 Introduction

In the permanent magnet synchronous motor (PMSM), cogging torque is inherently generated by the interaction between the magnetic field from the permanent magnets (PM) and teeth geometry [1,2]. It is a source of the noise and vibration of the PMSM and it often works a principal source of torque ripple. Also, it is difficult to control in the PMSM problems [3,4]. For that reason, many methods are studied to reduce the cogging torque in the laboratory. Earlier researchers have been proposed to reduce the cogging torque through a design of the stator structure, and the wave of surface flux density is not investigated due to uncertain magnetization in the ring-type PM. In order to enhance the quality of the machine, researchers have been used the optimization of the motor shape. The object of these studies was to have the sinusoidal air-gap flux density distribution. In other word, to change the position of permanent magnet or the structure of stator is a procedure for making a sinusoidal wave of flux density through adjusting the amount of flux from permanent magnet.

The magnetization direction in the case of ring-type PMSM is crucial because the position or the structure of PM cannot be modified. Moreover, the uncertain magnetization of the PM caused fairly often problem in the ring-type PM in industry.

The uncertain magnetization of the PM in the PMSM generates the additional slot harmonics. The addition of this slot harmonic has contributed to the considerably increase the total harmonic distortion (THD) of the back electromotive force (EMF) and the cogging torque. In particular, variation of the material properties influence on the back EMF which is an important response of the motors, furthermore, products cannot meet the required performances at times. Thus, in this study, the method to have the sinusoidal air-gap flux density distribution of magnetizing fixture is proposed. Besides, in order to optimize the magnetization in the PM, this paper presents a Taguchi robust design of the air-gap flux density characteristic analysis using the structural optimization of magnetizing fixture.

We investigated numerically and experimentally the uncertain magnetization of PM due to the design of magnetizing fixture and its effect on the air gap flux density.

Finally, the analysis result is verified through comparison of the optimum design model and present design model.

Item(motor)	*Unit*	*Values*
Number of the pole	-	8
Number of the slot	-	12
Rated power	[W]	80
Rated Speed	[rpm]	3000
DC-link voltage	[V]	12
Item(Magnetization)	*Unit*	*Values*
Number of turns	[turn]	5
Magnetizing voltage	[V]	2000

Table 1: Specification of the analysis model

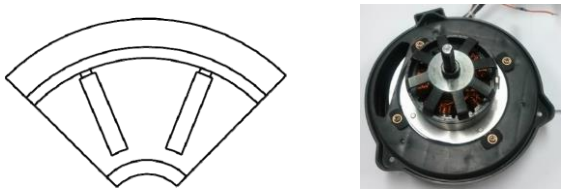

(a) (b)

Figure 1: Configuration of the magnetizing fixture and motor

2 Method of Analysis

The numerical procedure of this study is consisted of two steps. First, the magnetization of PM is determined by solving the equation for analyzing the magnetic field distribution, and differential electric circuit equations for the capacitor discharge magnetizer simultaneously. In the second step, the characteristic of the analysis model is confirmed.

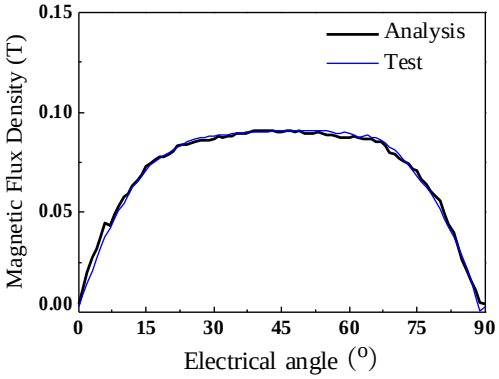

Figure 2: Surface flux density of the test and analysis result

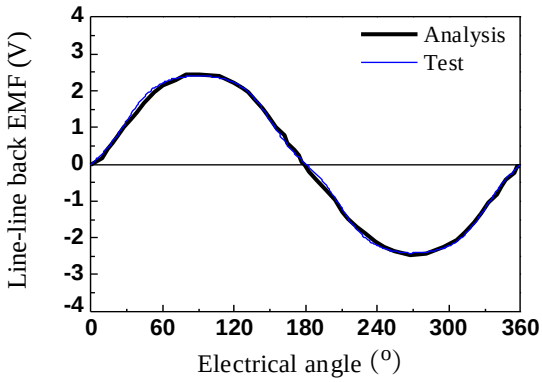

Figure 4: Line-line back EMF waveforms at 1000rpm

2.1 Analysis model

The cross-section view of the magnetizing fixture and analysis motor are shown in Fig. 1. The rated power and rated speed are 80W and 3000rpm respectively. The detail

specification of this magnetizing fixture and motor are listed in table 1. The magnetizing current was calculated by solving the differential equations of equivalent circuit of magnetizer [2].

2.2 Analysis theory

The governing equation for analyzing the magnetic field distribution of the magnetizing fixture is given by (1) [5].

$$\frac{\partial}{\partial x}\left(\frac{1}{\mu}\frac{\partial A_z}{\partial x}\right)+\frac{\partial}{\partial x}\left(\frac{1}{\mu}\frac{\partial A_z}{\partial y}\right) = -J_o-\frac{1}{\mu_o}\left(\frac{\partial M_y}{\partial x}-\frac{\partial M_x}{\partial y}\right)+\sigma\frac{\partial A_z}{\partial t} \quad (1)$$

where A_z is the z-component of magnetic vector potential, $1/\mu$ is magnetic resistivity, $1/\mu_0$ is magnetic resistivity of vacuum, and M_x, M_y are the x- and y-direction component of magnetization M of the permanent magnets for orientation. From the analysis of the magnetizing fixture, the flux density vectors $B_x^{(e)}$, $B_y^{(e)}$ of each element in PM region are obtained. The magnetization directions of the PM are arranged to same directions as internal flux, so the magnetization directions, $\theta^{(e)}$, the orientation for every element can be determined as

$$\theta^{(e)} = \tan^{-1}\frac{B_y^{(e)}}{B_x^{(e)}} \quad (2)$$

Figure 3: Testing apparatus for measuring the back EMF

For the elements of part of the magnet, the angles determined by Eq. (2) are output to a file as a database for the following magnetic field analysis. In short, we determined the magnitude of the residual magnetic flux density and magnetizing direction of PM by using the magnetization and demagnetization curves.

2.3 Reliability examination using experiments

The validity of the analysis method is verified by test. To confirm the state of magnetization, the two tests are carried out. First of all, the surface flux density of the motor is measured, and then, the line-line back EMF is measured at 1000rpm. Fig. 3 compares the measured values and the analytical values of the surface flux densities of the rotor. Both agree very well and show that the orientation of the

ring-type PM determined by this analysis is appropriate. Fig. 3 shows the testing apparatus that is used to measure the back EMF. The back EMF including harmonics can be expressed as a Fourier series as in

$$e_{ph} = \sum_{n=1}^{\infty} E_n \sin\left(n\frac{p}{2}\omega t\right) \quad (3)$$

where p is the number of poles and ω [rad/s] is the rotational angular speed of the rotor. E_n is the peak value of the nth harmonic of the back EMF. The result of comparing the back EMF between the analysis and measurement value at 1000 rpm is shown in Fig. 4. The validity of the analysis result is verified by comparing the test result in Fig. 2 and Fig. 4.

3 Magnetizing fixture optimum design

It is significant to design the magnetizing fixture because the quality of magnetization depends on the design of the magnetizing fixture. The important point in designing the magnetizing fixture is that the magnetic flux must flow sufficiently in ring-type PM. Additionally, the air gap flux density of the magnetizing fixture have to be sinusoidal as much as possible. That is because the air-gap flux density of the magnetizing fixture significantly influence on the back

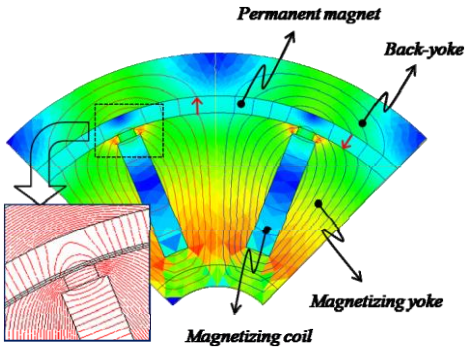

Figure 5: Path of magnetic flux in magnetizing fixture

EMF and cogging torque in the PMSM applied the ring-type PM. In this chapter, we introduce the model of magnetizing fixture, necessity of the robust design, and Taguchi method.

3.1 Model of magnetizing fixture

The path of magnetic flux in magnetizing fixture is shown in Fig. 5. The most important part of the ring-type PM is between pole and pole. So, this section is magnified as shown Fig. 5.

Fig. 6 shows a model of magnetizing fixture with an electromagnet which is classified as a six parameter problem. This is used to produce a square wave of the air gap flux density. The magnetizing fixture is set to form the flux distribution. The magnetic powder is inserted in the cavity. And then, the current is excited to each coil.

According to the configuration of the magnetizing fixture model, the flux distribution can be changed. Because it influences the performance of the magnets, it should be distributed as designer wants. In this model, the air gap flux density of the magnetizing fixture is specified as sinusoidal wave. Therefore, in order to be close to sinusoidal for flux density in the air gap, optimization for the magnetization in the PM is necessary. The sum of error between objective sinusoidal wave and analysis result in the air gap becomes the objective function of optimization. And it can be easily transformed as a robust design problem to reduce variation of the air gap flux density. Fig. 6 shows control factors. The selected control factors are listed in Table 2. In this study, Taguchi method is employed to obtain robust optimum design and detail is described in following section.

3.2 Taguchi method

Robust design technique which improves quality of products without reducing variances of performance can be a sort of solution [6,7]. Many robust optimization methods have been developed to minimize variances of the performances caused by tolerance. Among that, Taguchi robust design based on orthogonal array (OA) has been widely applied to various fields [8,9]. In original Taguchi robust design, experiments are performed as product of experimental point of inner array and outer array. Inner array is orthogonal array made up control factors and outer array is orthogonal array made up

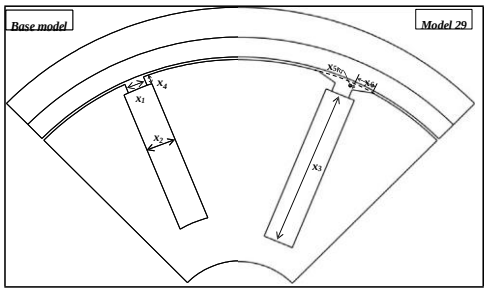

Figure 6: Control factors used in Taguchi robust design

Nos.	*Control factor*	*Units*	*Array pattern*		
			0	1	2
x_1	*slot opening*	[mm]	1.0	1.8	2.6
x_2	*slot width*	[mm]	3.0	4.0	5.0
x_3	*slot length*	[mm]	12.0	14.0	16.0
x_4	*tooth tip*	[mm]	0.9	1.2	1.5
x_5	*champer length*	[mm]	0.0	0.3	0.6
x_6	*champer width*	[mm]	0.0	2.0	4.0

Table 2: Selected control factors.

noise factors [10, 11]. But, in this model, noise factors are not considered. Instead of noise factors, outer array is filled with flux value at the regular interval points according to electrical angle. That's why it is eventually related with a distribution of the flux density. The flux is obtained from 18 points in the air gap and we use the L36 orthogonal array for control factors (6 variables with 3 levels) and the L18 outer array (18 points). Finally, the experiments are performed as listed in Table 3.

In the Taguchi method, a quadratic loss function to represent robustness as

$$L(f) = k(f - m)^2 \tag{4}$$

where k is the constant to define the loss and m is the target vale. The expected value of the loss function is defined as

$$Q = E[L(f)] = k[\sigma^2 + (\mu - m)^2] \tag{5}$$

where μ is the mean of f and σ is the standard deviation of f. The symbol f represents the response or objective function in a general design, while the symbol y is used for f in the Taguchi method. When the target value of a response is given, the Taguchi method determines the optimum setting of control factors, so that the variation of a response is minimized, although uncontrollable factors, called noise factors, exist. Eq. (5) can be regarded as the index to find a robust design. Suppose that we have a scale factor s to adjust the current mean to the target value. The scale factor s is described as

$$s = \frac{m}{\mu} \tag{6}$$

when the current mean is adjusted to the target value, the average loss function of (6) is changed to

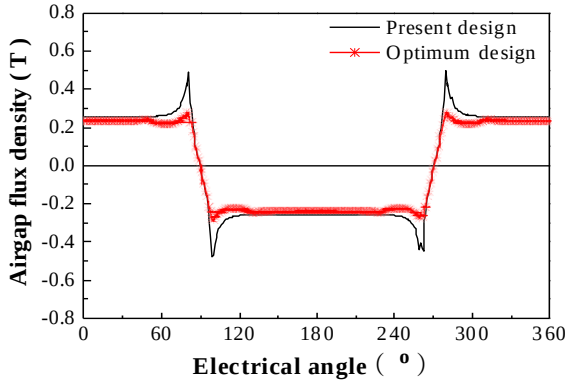

Figure 7: Comparison of the air gap flux density in the magnetizing fixture

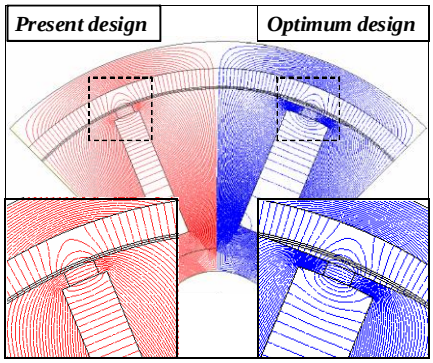

Figure 8: Comparison of the equi-potential line in the magnetizing fixture

$$Q_a = k\left[\left(\frac{m}{\mu} - m\right)^2 + \left(\frac{m}{\mu}\sigma\right)^2\right] = km^2\frac{\sigma^2}{\mu^2} \quad (7)$$

To enhance additivity of the effect on the control factors, (7) is transformed to

$$\eta = 10\log_{10}\frac{\mu^2}{\sigma^2} \quad (8)$$

Equation (8) is the ratio of the power of the signal factor μ and the power of noise factors σ. Thus, it is called the S/N ratio. Maximizing (8) is equivalent to minimizing (7). That is, a robust design is obtained by maximizing (8).

Taguchi robust design selects the best combination out of inner orthogonal array using SN-ratio [12]. Finally we apply ANOVA (analysis of variance) to expect the untested combination except to tested combination of inner orthogonal array.

4 Validation of optimization result

In order to expect untested combination, analysis of variance (ANOVA) is conducted and we find optimal combination out of all capable combinations. ANOVA is a statistical test for heterogeneity of means by analysis of group variances and it tests effects of each variable for response. The result of ANOVA is shown in Table 4.The slot width and champer

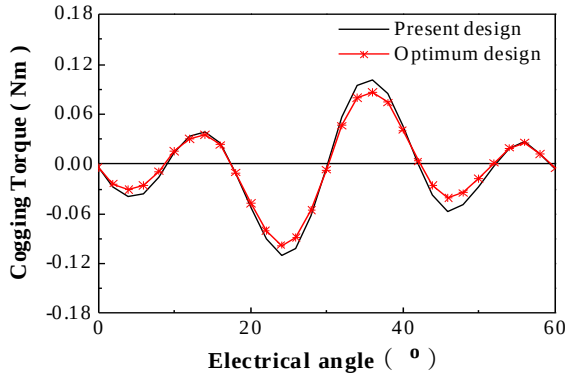

Figure 9: Comparison of the cogging torque waveform in the motor

width are better in high level and the slot opening, slot length, tooth tip, and champer length are better in middle level. The optimum combination of Taguchi robust design is shown in Table 5. To validate the result of Taguchi robust design, additional experiments of optimal design are performed. Fig. 7 presents the air gap flux density as the electrical angle with respected to the optimal magnetizing fixture that provides decrease. The comparison of the equi-potential line in the magnetizing fixture is shown in Fig. 8. Finally, the optimal results compared with present design and total experiments are shown in Table 6. The comparison of the cogging torque waveform in the motor is shown in Fig. 9. Because of the air-gap sinusoidal flux density in the magnetizing fixture, the cogging torque and THD of the back EMF is reduced.

5 Conclusion

This paper presents a Taguchi robust design of the surface flux density characteristic analysis using the structural optimization of magnetizing fixture. The optimization technique based on the Taguchi method has the advantages as follows:

1) The robust design method to have the sinusoidal flux density distribution in the air-gap of magnetizing fixture is proposed.

2) Optimum design model is accomplished by the proposed approach that performance of the motor is improved as compared with that of the present design.

Therefore, it is expected that the proposed design method can be improved in the quality of the product and reduction of the cost in mass production are the expected applications of this study.

Acknowledgements

This research was supported by the MSIP (Ministry of Science, ICT & Future Planning), Korea, under the CITRC (Convergence Information Technology Re-search Center) support programme (NIPA-2013-H0401-13-1008) supervised by the NIPA (National IT Industry Promotion Agency).

References

[1] J. Y. Lee, S. H. Lee, G. H. Lee, J. P. Hong , and J. Hur. "Determination of parameters considering magnetic nonlinearity in an interior permanent magnet synchronous motor," *IEEE Trans. Magn.*, **volume** 42, no.4, pp. 1303-1306, (2006).

[2] C. J. Lee, and G. H. Jang, "Development of a new magnetizing Fixture for the Permanent Magnet Brushless DC Motors to Reduce the Cogging Torque," *T IEEE Trans. Magn.*, **volume** 47, no.10, pp. 2410-2413, (2011).

[3] A. Hartman and W, Lorimer, "Undriven vibrations in brushless DC motors," *IEEE Trans. Magn.*, **volume** 37, no.2, pp. 789-792, (2001).

[4] Z. Azar, Z. Q. Zhu, and G. Ombach, "Influence of Electric Loading and Magnetic Saturation on Cogging Torque, Back-EMF and Torque Ripple of PM Macines," *IEEE Trans. Magn.*, **volume** 48, no.10, pp. 2650-2658, (2012).

[5] N. Takahashi, 'Finite element method in electrical engineering,' (Morikita Publishing Co., 1986, 2nd edn.).

[6] Y. K. Kim, J. P. Hong, and J. Hur, "Torque Characteristic Analysis considering the Manufacturing Tolerance for Electric Machine by Stochastic Response Surface Method," *IEEE Trans. Magn.*, **volume** 39, no. 3, pp. 713-719, (2003).

[7] S. J. Lee, K. S Kim, S. Cho, J. Jang, T. H. Lee ,and J. P. Hong, "Optimal Design of Interior Permanent Magnet Synchronous Motor considering the Manufacturing Tolerances using Taguchi Robust Design," *IET Electr. Power Appl.*, **volume** 8, no.1, pp. 23-28, (2014).

[8] G. Taguchi, and Y. Wu, '*Introduction to Off-Lin Quality Control*, Central Japan Quality Control Association (available from American Supplier Institute, 32100 Detroit Industrial Expressway, Romulus, MI 48174),' (1980).

[9] G. Park, T. LEE, K.H. Lee, H. Hwang, "Robust Design: An Overview," *AIAA Journal*, **volume** 44, no.1, pp. 181-191, (2006).

[10] G. Taguchi, Y. Yokoyama and Y. Wu, '*Taguchi methods – design of experiments*,' (American Supplier Institute, Inc, Press., 1983.).

[11] N. Takahashi, K. Ebihara, K. Yoshida, T. Nakata, K. Ohashi, and K. Miyata, "Investigation of simulated annealing method and its application to optimal design of die mold for orientation of magnetic powder," *IEEE Trans. Magn.*, **volume** 326, no.3, pp. 1210-1213, (1996).

[12] M. A. Tsili, E. I. Amoiralis, A. G. Kladas, A. T. Sourlaris, "Optimal Design of Multi-winding Transformer using Combined FEM, Taguchi and Stochastic-Deterministic Approach," *IET Electr. Power Appl.*, **volume** 6, no.7, pp. 23-28, (2012).

Number	**Control factor**						**Outer array**				
	Array pattern						**Electrical andgle**				
	slot opening	***slot width***	***slot length***	***tooth tip***	***champer length***	***champer width***	0◦	10◦		160◦	170◦
L01	0	0	0	0	0	0	1	2		17	18
L02	1	1	1	1	1	1	19	20		35	36
L03	2	2	2	2	2	2	37	38	~	53	54
L04	0	0	0	0	1	1	55	56		71	72
L05	1	1	1	1	2	2	73	74		89	90
			~						~		
L30	2	1	0	0	0	2	523	524		539	540
L31	0	2	2	2	1	2	541	542		557	558
L32	1	0	0	0	2	0	559	560		575	576
L33	2	1	1	1	0	1	577	578	~	593	594
L34	0	2	0	1	2	1	595	560		611	612
L35	1	0	1	2	0	2	613	614		629	630
L36	2	1	2	0	1	0	631	632		647	648

Table 3: Taguchi orthogonal array with inner array and out array from measurement point.

Factor	*Degree of freedom*	*Level*			*Sum of square*	*Mean of square sum*	*Contribution (%)*	*F ratio*	*p-value*	*Standard F ratio*
		0	*1*	*2*						*F(0.01,2,57)*
slot opening	2	6.7309	7.5422	5.5479	24.1387	12.0693	40.5360	14.7041	0.0002	2.4609
slot width	2	6.5553	6.0648	7.2010	7.7940	3.8970	13.0884	4.7477	0.0230	2.4609
slot length	2	6.2995	6.8663	6.6551	1.9690	0.9845	3.3066	1.1994	0.3256	2.4609
tooth tip	2	6.7731	6.9178	6.1301	4.2188	2.1094	7.0847	2.5699	0.1059	2.4609
champer length	2	6.5118	6.6838	6.6253	0.1836	0.0918	0.3083	0.1118	0.8948	2.4609
champer width	2	6.2587	6.6941	6.8682	2.3660	1.1830	3.9731	1.4412	0.2641	2.4609
Error	23									
Total	35						100			

Table 4: ANOVA (ANOVA of control factors).

Factor	*slot opening*	*slot width*	*slot length*	*tooth tip*	*champer length*	*champer width*
Optimum (level)	1	2	1	1	1	2

Table 5: Optimum conditions of Taguchi robust design.

Estimation	*Back EMF [V]*		*Cogging torque*
	rms	*THD*	
present design	*1.550*	*2.188*	0.212
Optimum design	*1.528*	*2.045*	0.187
Improvement %	-	*6.536*	11.79

Table 6: Comparison between present design and optimum design.